А С Т Р О Ф И З И К А

ТОМ 64 ФЕВРАЛЬ, 2021 ВЫПУСК 1

SOBOLEV LVG ANALYSIS OF PREBIOTIC MOLECULE FORMAMIDE (NH_2CHO) FOUND IN THE ISM

M.K.SHARMA[1], V.D.MAMPATTA[1], M.SHARMA[2], S.CHANDRA[1]

Received 16 May 2019

Accepted 23 December 2020

Using known values of rotational and centrifugal distortion constants in conjunction with electric dipole moment of NH_2CHO, we have calculated energies of rotational levels in the ground vibrational state, and the probabilities for radiative transitions between the levels. The radiative transition probabilities in conjunction with the scaled values of collisional rate coefficients are used in the Sobolev LVG analysis of NH_2CHO. There are some strong lines. For ortho-NH_2CHO, we have found one transition 1_{10}-1_{11} showing anomalous absorption and five transitions 6_{15}-5_{14}, 7_{17}-6_{16}, 7_{16}-6_{15}, 8_{18}-7_{17}, 8_{17}-7_{16} showing emission feature. For para-NH_2CHO, six emission transitions 5_{05}-4_{04}, 6_{06}-5_{05}, 7_{07}-6_{06}, 8_{08}-7_{07}, 9_{09}-8_{08}, $10_{0,10}$-9_{09} are found. Out of these 12 transitions, three transitions, 1_{10}-1_{11}, 5_{05}-4_{04}, and 8_{08}-7_{07}, are already found in the ISM. Other relatively weaker lines are also found in the ISM. In addition to the observed lines, 9 transitions may play important role in the identification of NH_2CHO in a cosmic object.

Keywords: *ISM: molecules: NH_2CHO: Einstein A coefficients: radiative transfer*

1. *Introduction.* Formamide is a characteristic hot core molecule which is quite ubiquitous in the interstellar medium (ISM). In the ISM, the most abundant triatomic inorganic molecule is the H_2O and the organic molecule is the HCN. Combination of these two molecules gives the formamide (NH_2CHO).

$$H_2O + HCN \rightarrow NH_2CHO . \qquad (1)$$

Hence, we may say that the NH_2CHO is quite abundant in the ISM. The formamide plays a vital role in the prebiotic chemistry because it not only has amide linkage within it but also has four out of six elements (carbon, nitrogen, hydrogen, oxygen) which are common in all life forms [1]. Formamide also acts as a multifunctional prebiotic cursor because of its capability to produce a panel of low molecular weight compounds upon partial degradation, which later acts as intermediates for the synthesis of bio-molecules (nucleic acids) and thereby increasing the network of possible transformations [2]. Formamide may be considered as the origin point for the prebiotic synthesis of both metabolic and genetic species like amino acids, nucleic acid bases, sugars, and carboxylic acids.

For a colossal period of time, the prebiotic importance of formamide was hampered to the synthesis of adenine alone [3,4]. Gentle heating of NH_2CHO at 160° C in the presence of catalytic amounts of alumina (Al_2O_3), calcium carbonate ($CaCO_3$), silica (SiO_2), and zeolite (Y type) yielded cytosine and 4(3H)-pyrimidinone, alongside adenine and purine [5]. Thymine and adenine were produced from NH_2CHO in the presence of titanium dioxide (TiO_2) [6]. Uracil, cytosine, adenine and hypoxanthine were obtained by the thermal condensation of NH_2CHO in the presence of clays of the montmorillonite family [7]. Adenine, cytosine and uracil were obtained by warming NH_2CHO in the presence of mineral phosphates [8,9]. The guanine is also synthesized from NH_2CHO by a combined UV-irradiation/thermal condensation process in the presence of phosphate minerals [10]. Irradiation (UV light) of NH_2CHO on the surface of a TiO_2 (001) single crystal at low temperature in ultra-high vacuum conditions showed the formation of all five nucleic bases [11]. The isocytosine, cytosine, adenine and uracil are synthesized from NH_2CHO and borate minerals [12]. Finally, in interstellar conditions, uracil, isocytosine and adenine are synthesized by heat driven condensation of NH_2CHO in the presence of Murchison material (meteorite) [13]. The peptide bond, -C(=O)NH- plays an important role in holding together chains of amino acids. A recent study [14] states that out of all possible simplest interstellar molecules having a peptide bond, formamide is having more stability energy wise.

It is a planar molecule with electric dipole moment having components $\mu_a = 2.7$ Debye and $\mu_b = 0.85$ Debye [23], showing that *a*-type transitions are much stronger than the *b*-types. Therefore, in the present investigation, we have considered *a*-type transitions.

In the ISM, the first detection of formamide was made by Rubin et al. [16] through the transition $2_{11} \rightarrow 2_{12}$ towards the direction of Sgr B2. Then, Gottlieb et al. [17] found formamide towards Sgr A through its transition 1_{11}-1_{10}. Other *a*-type transitions of formamide found in the ISM are, 4_{13}-3_{12}, 5_{15}-4_{14}, 5_{14}-4_{13}, 5_{05}-4_{04}, 5_{32}-4_{31}, 7_{34}-6_{33}, 8_{35}-7_{34}, 10_{19}-9_{18}, 12_{58}-11_{57}, 4_{04}-3_{03}, 4_{22}-3_{21}, 5_{23}-4_{22}, 7_{25}-6_{24}, 7_{26}-6_{25}, 7_{44}-6_{43}, 8_{08}-7_{07}, 10_{29}-9_{28}, 11_{29}-10_{28}, $11_{2.10}$-10_{29} [18,19]. Though the μ_b is very small, the *b*-type transitions, $16_{3.14}$-$16_{2.15}$, 8_{27}-7_{16}, $17_{3.15}$-$17_{2.16}$, $34_{3.31}$-$34_{2.32}$, $18_{3.16}$-$18_{2.17}$, $28_{4.24}$-$28_{3.25}$, $19_{3.17}$-$19_{2.18}$, $20_{3.18}$-$20_{2.19}$, $20_{1.19}$-$19_{2.18}$ are found by Coutens et al. [20].

Because of its importance, the NH_2CHO has been studied in terrestrial laboratories from time to time [15,21-23]. In the present investigation, we have used the rotational and centrifugal distortion constants of Motiyenko et al. [23] derived in the S-reductions of Watson Hamiltonian in I^r representation, given in Table 1 (column 2). They have also derived the constants in A-reduction. We have also optimized the formamide with the help of the software GAUSSIAN 2009, where we have used B3LYP method, and aug-cc-pVDz and aug-cc-pVTz basis sets. The rotational and centrifugal distortion constants thus obtained, are given in columns 3 and 4 of Table 1. The coordinates of the constituent atoms of NH_2CHO are given in Table 2.

Table 1

ROTATIONAL AND CENTRIFUGAL DISTORTION CONSTANTS OF NH_2CHO IN MHz

Constant	Experiment	aug-cc-pVDZ	aug-cc-pVTZ
A	72716.89840 (19)	68917.7431	69897.7677
B	11373.509642 (28)	11792.3951	11827.5278
C	9833.952804 (27)	10069.4321	10115.8128
$D_J \cdot 10^3$	7.761879 (23)	8.660732	8.758405
$D_{JK} \cdot 10^3$	-67.83261 (43)	-4.090403	2.360077
$D_K \cdot 10^3$	1400.6906 (38)	1710.978520	1822.174884
$d_1 \cdot 10^3$	1.5757698 (38)	-1.653967	-1.640637
$d_2 \cdot 10^3$	0.1116821 (18)	-0.167524	-0.172708
$H_J \cdot 10^9$	9.3375 (57)	1.640266469	1.530744346
$H_{JK} \cdot 10^6$	-0.19637 (18)	-7.078574333	-7.099341329
$H_{KJ} \cdot 10^6$	-5.7948 (20)	114.5500560	127.7877675
$H_K \cdot 10^6$	80.679 (48)	-0.3172925461	-0.3319796552
$h_1 \cdot 10^9$	4.5512 (18)	4.080127967	4.125254139
$h_2 \cdot 10^9$	0.8207 (16)	0.9139578507	0.9532567955
$h_3 \cdot 10^9$	0.17663 (30)	0.2675426213	0.2783410987
$L_{JK} \cdot 10^9$	-0.01208 (49)		
$L_{KKJ} \cdot 10^9$	0.4272 (29)		
$L_K \cdot 10^9$	-5.41 (16)		
$l_2 \cdot 10^{12}$	-0.01296 (26)		

Table 2

STRUCTURE OF NH_2CHO MOLECULE

Atom	Coordinates (Å)		
	x	y	z
N	0.000000	0.533591	0.000000
H	-1.827698	0.131735	0.000000
H	1.994731	0.641477	0.000000
C	1.138419	-0.018162	0.000000
H	1.271245	-1.096833	0.000000
O	-1.033599	-0.412817	0.000000

Owing to the pair of hydrogen atoms, the rotational levels are classified into two distinct groups: ortho species having odd values of k_a and para species having even values of k_a. For known values of rotational and centrifugal distortion constants in conjunction with electric dipole moment μ_a of NH_2CHO, we have calculated energies of rotational levels, and the probabilities for radiative transitions between the levels. The radiative transition probabilities in conjunction with the scaled values of collisional rate coefficients are used in the Sobolev Large Velocity

Gradient (LVG) analysis of NH_2CHO. Among the strongest transitions, for ortho-NH_2CHO, we have found one transition showing anomalous absorption and five transitions showing emission feature, whereas for the para-NH_2CHO, six emission transitions are found. Out of these transitions, 3 are already found in the ISM. In addition to the observed lines, 9 transitions may play important role in the identification of NH_2CHO in a cosmic object.

2. *Radiative transitions*. The *a*-type radiative transitions between rotational levels are governed through the selection rules:

$$\begin{aligned} &J: \quad \Delta J = 0, \pm 1 \\ &k_a, k_c: \quad \text{odd, even} \leftrightarrow \text{odd, odd} \quad (\text{ortho transition}) \\ &\qquad\quad \text{even, even} \leftrightarrow \text{even, odd} \quad (\text{para transition}). \end{aligned}$$

For each of the ortho and para species, we have considered 120 rotational levels. For ortho species, the levels are up to 173 cm^{-1} connected through 440 radiative transitions, whereas for the para species, the levels are up to 171 cm^{-1} connected through 446 radiative transitions. Using the experimental values of rotational and centrifugal distortion constants, and electric dipole moment μ_a, the energies of levels and radiative transition probabilities are calculated with the help of the software ASROT [24].

3. *Collisional transitions*. Besides the radiative transitions, the levels are connected through the collisional transitions. Though the collisional transitions do not follow any selection rules, the calculation of collisional rate coefficients is a difficult task [25-27]. Hence, we have used some scaled values of collisional rate coefficients. These values are calculated using the method discussed by Sharma et al. [28-30]. The background temperature of the cosmic microwave background is $T_{bg} = 2.73$ K. The LVG analysis is carried out in accordance with the procedure discussed by Sharma et al. [28-30].

4. *Model*. In the Large Velocity Gradient (LVG) analysis, a set of statistical equilibrium equations coupled with the equations of radiative transfer is written as the following.

$$n_i \sum_{\substack{j=1 \\ j \neq i}}^{120} P_{ij} = \sum_{\substack{j=1 \\ j \neq i}}^{120} n_i P_{ji} \qquad i = 1, 2, ..., 120 \tag{2}$$

where n denotes the population density of energy level and the parameter P is as the following.

(i) For a radiatively allowed transition

$$P_{ij} = \begin{cases} \left(A_{ij} + B_{ij} I_{v,bg}\right)\beta_{ij} + n_{H_2} C_{ij} & i > j \\ B_{ij} I_{v,bg}\, \beta_{ij} + n_{H_2} C_{ij} & i < j \end{cases}$$

(ii) For a radiatively forbidden transition

$$P_{ij} = n_{H_2} C_{ij} \,.$$

Here, A and B are the Einstein coefficients, C the rate coefficient for collisional transition and n_{H_2} the density of molecular hydrogen. The escape probability β for the transition is

$$\beta_{lu} = \beta_{ul} = \frac{1-\exp(-\tau_\nu)}{\tau_\nu},$$

where optical depth τ_ν is expressed as

$$\tau_\nu = \frac{hc}{4\pi(d\,v_r/dr)}\left[B_{lu}n_l - B_{ul}n_u\right],$$

where $(d\,v_r/dr)$ denotes the velocity gradient in the region. This is non-linear set of equations.

The external radiation field impinging on the volume element, generating the lines, is the cosmic microwave background (CMB) only, which corresponds to the background temperature $T_{bg} = 2.73$ K. The parameter γ is expressed as

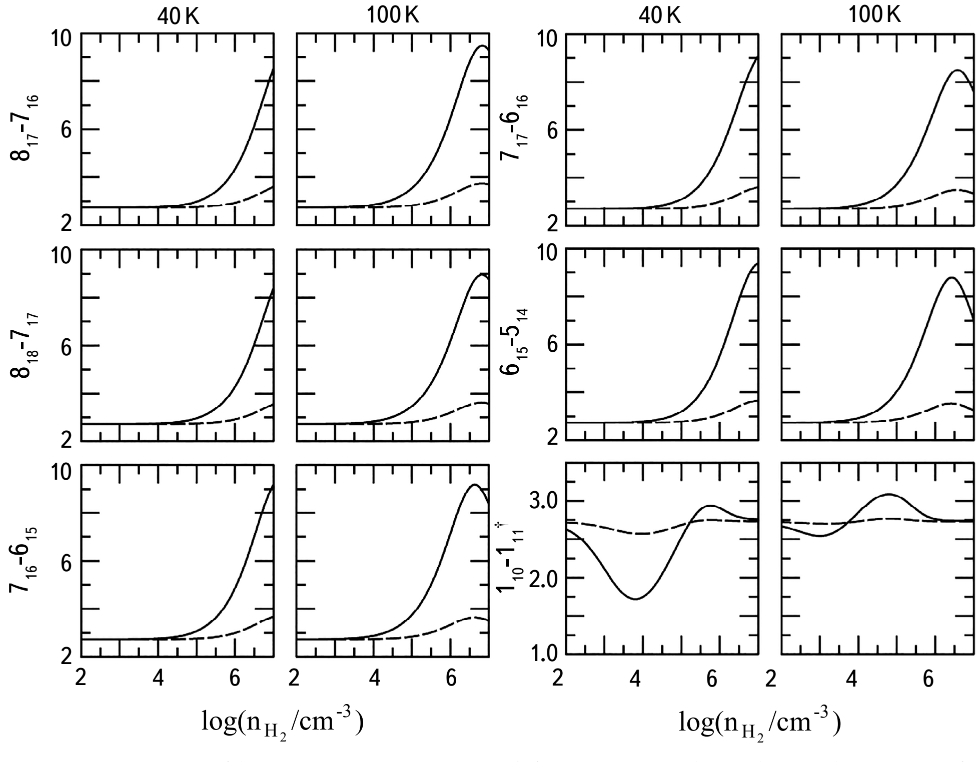

Fig.1. Variation of brightness temperatures T_B (K) versus molecular hydrogen density n_{H_2} for kinetic temperatures 40 and 100 K (written at the top) for six ortho transitions (written on the left) of NH_2CHO. Solid line is for $\gamma = 10^{-5}$ cm^{-3} (km/s)$^{-1}$ pc, and dotted line for $\gamma = 10^{-6}$ cm^{-3} (km/s)$^{-1}$ pc. Observed line is denoted by †.

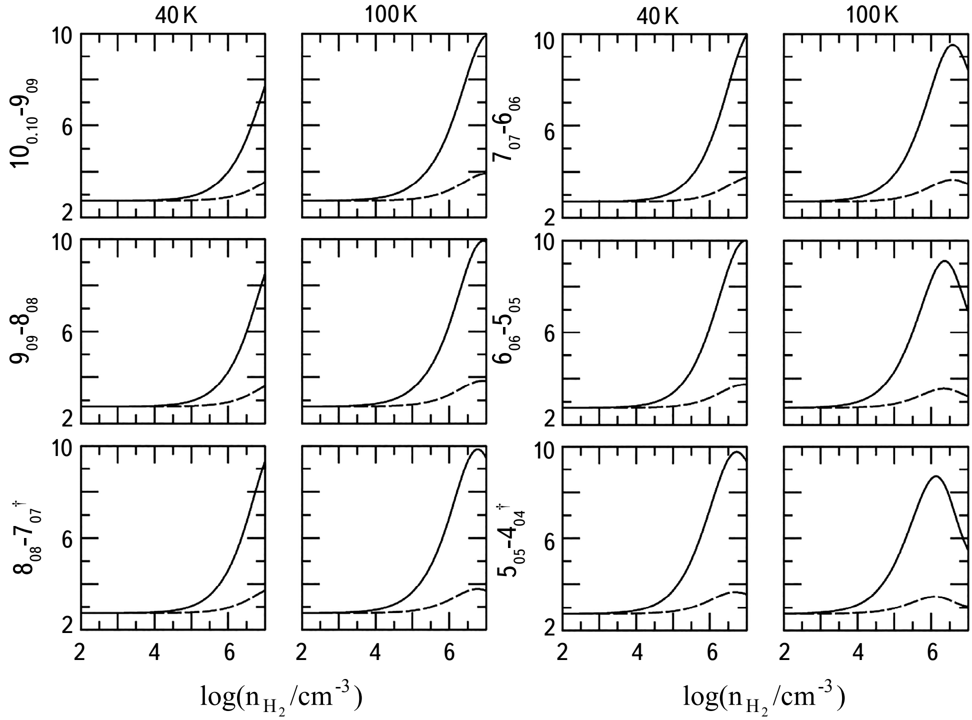

Fig.2. Same as Fig.1, but for six para transitions (written on the left) of NH_2CHO.

Table 3

FREQUENCY ν, EINSTEIN A-COEFFICIENT A_{ul}, ENERGY E_u OF UPPER LEVEL, RADIATIVE LIFE-TIME t_u OF UPPER LEVEL AND t_l OF LOWER LEVEL FOR TRANSITION

Transition	ν (MHz)	A_{ul} (s^{-1})	E_u (cm^{-1})	t_u (s)	t_l (s)
1_{10}-1_{11}	1539.569	$2.768 \cdot 10^{-10}$	2.8029706114	$3.61 \cdot 10^{9}$	∞
6_{15}-5_{14}	131620.401	$1.552 \cdot 10^{-4}$	17.4394042223	$6.44 \cdot 10^{3}$	$1.14 \cdot 10^{4}$
7_{17}-6_{16}	142696.619	$2.014 \cdot 10^{-4}$	21.1190145030	$4.97 \cdot 10^{3}$	$8.01 \cdot 10^{3}$
7_{16}-6_{15}	153435.988	$2.504 \cdot 10^{-4}$	22.5539371688	$3.99 \cdot 10^{3}$	$6.44 \cdot 10^{3}$
$8_{1.8}$-$7_{1.7}$	162951.459	$3.039 \cdot 10^{-4}$	26.5507298012	$3.29 \cdot 10^{3}$	$4.97 \cdot 10^{3}$
$8_{1.7}$-7_{16}	175190.823	$3.776 \cdot 10^{-4}$	28.3936312768	$2.65 \cdot 10^{3}$	$3.99 \cdot 10^{3}$
5_{05}-4_{04}	105463.870	$8.081 \cdot 10^{-5}$	10.5702233953	$1.24 \cdot 10^{4}$	$2.46 \cdot 10^{4}$
6_{06}-5_{05}	126246.790	$1.407 \cdot 10^{-4}$	14.7784497182	$7.11 \cdot 10^{3}$	$1.24 \cdot 10^{4}$
$7_{0.7}$-6_{06}	146869.617	$2.239 \cdot 10^{-4}$	19.6741036029	$4.47 \cdot 10^{3}$	$7.11 \cdot 10^{3}$
8_{08}-7_{07}	167317.144	$3.336 \cdot 10^{-4}$	25.2513417429	$3.00 \cdot 10^{3}$	$4.47 \cdot 10^{3}$
$9_{0.9}$-$8_{0.8}$	187582.562	$4.730 \cdot 10^{-4}$	31.5040938197	$2.11 \cdot 10^{3}$	$3.00 \cdot 10^{3}$
$10_{0.10}$-$9_{0.9}$	207669.073	$6.449 \cdot 10^{-4}$	38.4263962419	$1.55 \cdot 10^{3}$	$2.11 \cdot 10^{3}$

$\gamma = n_{mol} / (d\,v_r / dr)$. Here, n_{mol} is the density of the species of formamide and $(d\,v_r / dr)$ the velocity gradient in the object. Equation (2) is a set of homogeneous equations which does not have unique solution. In order to make the set of equations inhomogeneous, the last statistical equilibrium equation is replaced by the following equation, showing conservation.

$$\sum_{i=1}^{120} n_i = n_{mol} ,$$

where n_{mol} is the density of NH_2CHO molecule in the region. Using the values of radiative and collisional transition probabilities, each set of non-linear equations is solved through iterative procedure where the initial population densities of levels are taken as the thermal populations, corresponding to the kinetic temperature.

5. *Results and discussion*. For each of the ortho and para species of formamide, we have considered a set of 120 rotational levels connected by radiative and collisional transitions. The LVG analysis is performed using wide range of physical parameters in order to include a large number of cosmic objects where formamide could be detected. The molecular hydrogen density n_{H_2} is taken from 10^2 to $10^7\,cm^{-3}$. The kinetic temperatures T are 20, 40, 60, 80 and 100 K. However, in figures we have given the values for 40 and 100 K. The values of $\gamma[= n_{mol} / (d\,v_r / dr)]$

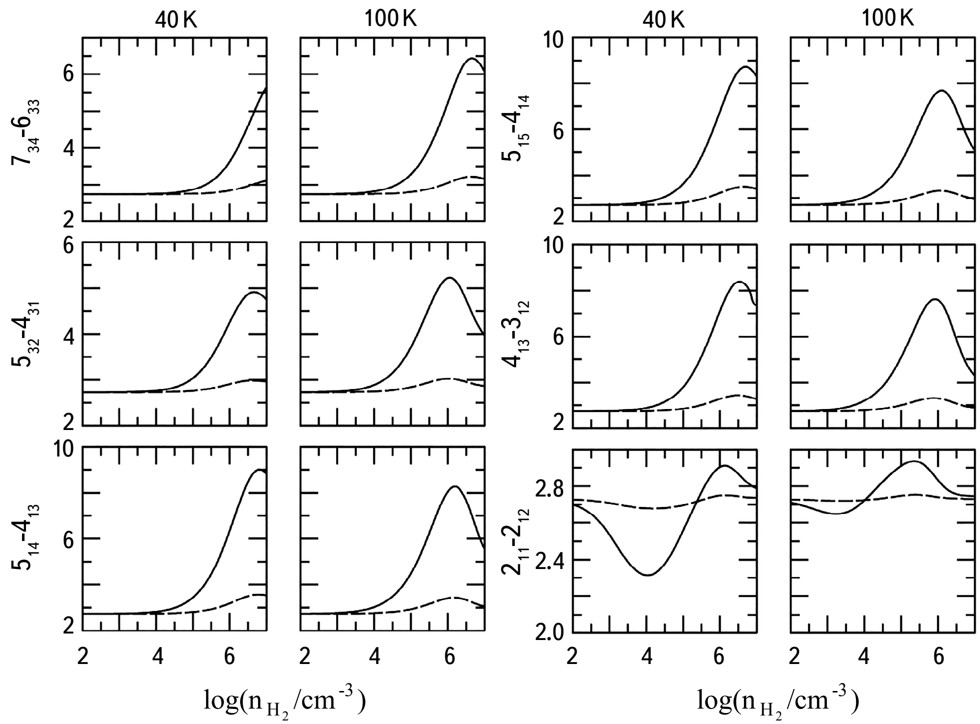

Fig.3. Same as Fig.1, but for six ortho observed transitions (written on the left) of NH_2CHO.

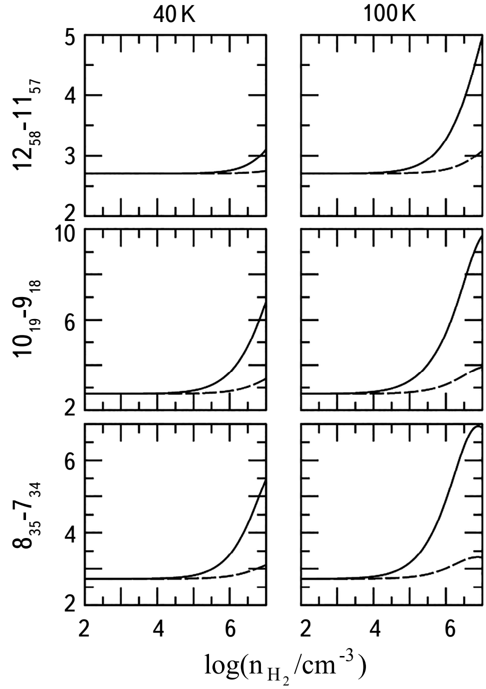

Fig.4. Same as Fig.1, but for three ortho observed transitions (written on the left) of NH_2CHO.

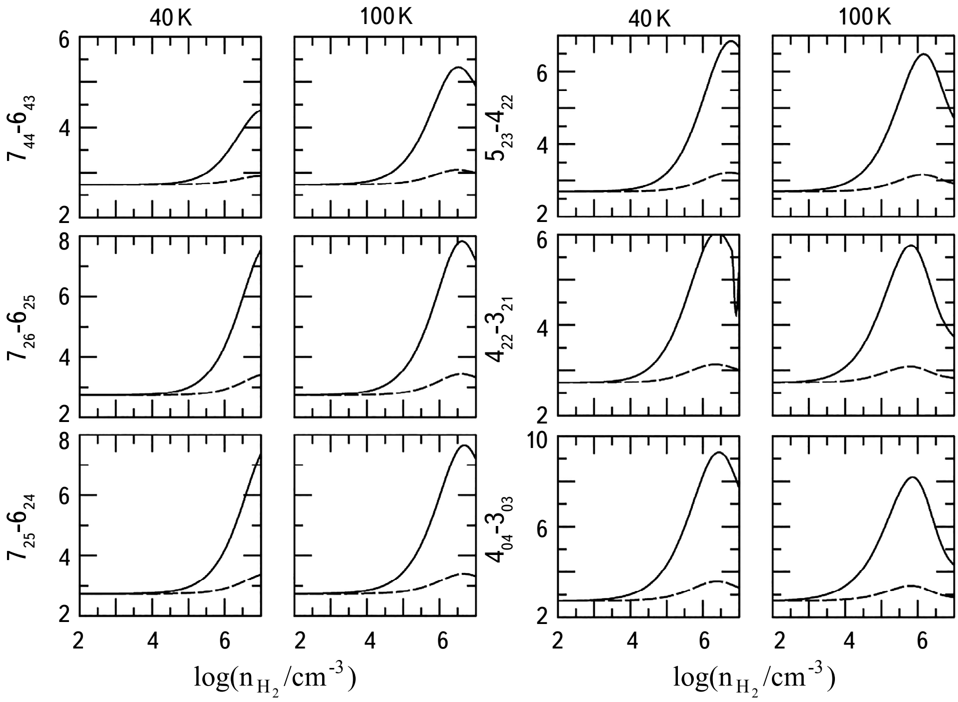

Fig.5. Same as Fig.1, but for six para observed transitions (written on the left) of NH_2CHO.

are taken as 10^{-5} and $10^{-6}\,\mathrm{cm}^{-3}\,(\mathrm{km/s})^{-1}$ pc. Here, n_{mol} denotes the density of NH_2CHO and dv_r/dr the velocity /background gradient in the region. The background corresponds to the temperature $T_{bg}=2.73$ K. A large number of lines are found to be produced. We have taken 6 strongest lines of each of the species.

Fig.1 shows the variations of brightness temperatures T_B (K) versus the density of molecular hydrogen n_{H_2} for the two kinetic temperatures 40 and 100 K (written on the top) for six ortho transitions, 1_{10}-1_{11}, 6_{15}-5_{14}, 7_{17}-6_{16}, 7_{16}-6_{15}, 8_{18}-7_{17}, 8_{17}-7_{16} (written on the left). The transition 1_{10}-1_{11} has been found in the ISM and shows the anomalous absorption. The rest five transitions are found to show emission feature. Fig.2 is the same as Fig.1, but for six para transitions, 5_{05}-4_{04}, 6_{06}-5_{05}, 7_{07}-6_{06}, 8_{08}-7_{07}, 9_{09}-8_{08}, $10_{0.10}$-9_{09}, showing emission feature. Out of them, two transitions, 5_{05}-4_{04} and 8_{08}-7_{07} are already found in the ISM. The details of these 12 transitions are given in Table 3. With the increase of kinetic temperature, for the absorption line 1_{10}-1_{11}. the depth of the trough is found to decrease and shift towards a lower density. All emission lines are found to show a peak in intensity. The position of the peak is found to shift towards a lower density with the increase of kinetic temperature.

Other 18 observed *a*-type lines are found to have relatively weak intensity. Results for these lines are given in Fig.3-6. The transition 2_{11}-2_{12} is found to show

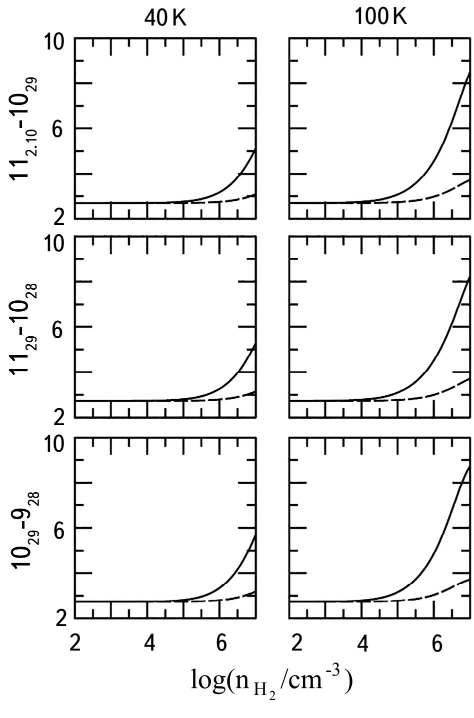

Fig.6. Same as Fig.1, but for three para observed transitions (written on the left) of NH_2CHO.

anomalous absorption whereas other 17 are found to show emission. In addition to 21 *a*-type observed lines, there are 9 strong lines which also may help in the identification of formamide in a cosmic object.

6. *Conclusions*. For each species, by solving a set of 120 statistical equilibrium equations coupled with the equations of radiative transfer, we find that there are 9 strong lines in addition to 21 observed *a*-type lines which may help in the detection of formamide in a cosmic object.

Acknowledgments. The author is grateful to learned Reviewers for encouraging and constructive comments. We are also grateful to Hon'ble Dr. Ashok K.Chauhan, Founder President, Hon'ble Dr. Atul Chauhan, Chancellor, Amity University and Prof. Dr. Balvinder Shukla, Vice-Chancellor, Amity University for valuable support and encouragements. MKS is thankful to the SERB, DST, New Delhi for awarding NPDF.

[1] Amity Center for Astronomy and Astrophysics, Amity Institute of Applied Sciences, Amity University, Noida 201313, U.P., India
[2] School of Studies in Physics, Jiwaji University, Gwalior 474011, M.P., India, e-mail: suresh492000@yahoo.co.in

СОБОЛЕВ LVG АНАЛИЗ ПРЕБИОТИЧЕСКОЙ МОЛЕКУЛЫ - ФОРМАМИДА (NH_2CHO), ОБНАРУЖЕННОЙ В ISM

М.К.ШАРМА[1], В.Д.МАМПАТТА[1], М.ШАРМА[2], С.ЧАНДРА[1]

Используя известные значения констант вращательного и центробежного дисторсий вместе с электрическим дипольным моментом NH_2CHO, мы рассчитали энергии вращательных уровней в основном колебательном состоянии и вероятности радиационных переходов между уровнями. В анализе NH_2CHO используются вероятности радиационных переходов вместе с масштабированными значениями коэффициентов скорости столкновений. Есть несколько сильных линий. Для орто- NH_2CHO мы нашли один переход 1_{10}-1_{11}, показывающий аномальное поглощение, и пять эмиссионных переходов 6_{15}-5_{14}, 7_{17}-6_{16}, 7_{16}-6_{15}, 8_{18}-7_{17}, 8_{17}-7_{16}. Для пара- NH_2CHO обнаружено шесть эмиссионных переходов 5_{05}-4_{04}, 6_{06}-5_{05}, 7_{07}-6_{06}, 8_{08}-7_{07}, 9_{09}-8_{08}, $10_{0,10}$-9_{09}. Из этих 12 переходов три перехода, $1_{10}-1_{11}$, $5_{05}-4_{04}$ и $8_{08}-7_{07}$, уже обнаружены в ISM. Другие относительно более слабые линии также встречаются в ISM. Помимо наблю-

даемых линий, 9 переходов могут играть важную роль в идентификации NH_2CHO в астрофизических объектах.

Ключевые слова: *молекулы: NH_2CHO: коэффициенты Эйнштейна А: перенос излучения*

REFERENCES

1. *R.Saladino*, *C.Crestini*, *G.Costanzo et al.*, Top. Curr. Chem., **259**, 29, 2005.
2. *V.S.Nguyen*, *H.L.Abbott*, *M.M.Dawley et al.*, J. Phys. Chem. A, **115**, 841, 2011.
3. *H.Bredereck*, *R.Gompper*, *H.G.V.Schuh et al.*, Angew. Chem., **71**, 753, 1959.
4. *T.Okamoto*, *M.Toshihiko*, *H.Yamada et al.*, Jpn Kokai Tokkyo Koho, **3**, 1, 1972.
5. *R.Saladino*, *C.Crestini*, *G.Costanzo et al.*, Bioorg. Med. Chem., **9**, 1249, 2001.
6. *R.Saladino*, *U.Ciambecchini*, *C.Crestini*, Chembiochem, **4**, 514, 2003.
7. *R.Saladino*, *C.Crestini*, *U.Ciambecchini et al.*, Chembiochem, **5**, 1558, 2004.
8. *R.Saladino*, *C.Crestini*, *V.Neri et al.*, Chembiochem, **7**, 1707, 2006.
9. *G.Costanzo*, *R.Saladino*, *C.Crestini et al.*, BMC Evol. Biol., **7**, 1, 2007.
10. *H.L.Barks*, *R.Buckley*, *G.A.Grieves*, Guanine, Chembiochem, **11**, 1240, 2010.
11. *S.D.Senanayake*, *H.Idriss*, Proc. Nat. Acad. Sci., **103**, 1194, 2006.
12. *R.Saladino*, *M.Barontini*, *C.Cossetti et al.*, Orig. Life. Evol. Biosph., **41**, 317, 2011.
13. *R.Saladino*, *C.Crestini*, *C.Cossetti et al.*, Orig. Life. Evol. Biosph., **41**, 437, 2011.
14. *M.Lattelais*, *F.Pauzat*, *Y.Ellinger et al.*, Astron. Astrophys., **519**, A30, 2010.
15. *R.J.Kurland*, *E.B.Wilson Jr*, J. Chem. Phys., **27**, 585, 1957.
16. *R.H.Rubin*, *G.W.Swenson Jr*, *R.C.Benson et al.*, Astrophys. J., **169**, L39, 1971.
17. *C.A.Gottlieb*, *P.Palmer*, *L.J.Rickard*, Astrophys. J., **182**, 699, 1973.
18. *C.Kahane*, *C.Ceccarelli*, *A.Faure et al.*, Astrophys. J. Lett., **763**, L38, 2013.
19. *V.Thiel*, *A.Belloche*, *K.M.Menten et al.*, Astron. Astrophys., **605**, L6, 2017.
20. *A.Coutens*, *J.K.Jrgensen*, *M.H.D. Van der Wiel et al.*, Astron. Astrophys., **590**, L6, 2016.
21. *R.J.Kurland*, J. Chem. Phys., **23**, 2202, 1955.
22. *C.C.Costain*, *J.M.Dowling*, J. Chem. Phys., **32**, 158, 1960.
23. *R.A.Motiyenko*, *B.Tercero*, *J.Cernicharo et al.*, Astron. Astrophys., **548**, A71, 2012.
24. *Z.Kisiel*, *J.Demaison et al.*, Spectroscopy from Space, PROSPE Programs for Rotational Spectroscopy, Kluwer Academic Publishers, Institute of Physics, Academy of Science, Warsaw, Dordrecht, 91, 2001.
25. *M.K.Sharma*, *M.Sharma*, *U.P.Verma et al.*, Adv. Space Res., **54**, 1963, 2014.
26. *M.Sharma*, *M.K.Sharma*, *U.P.Verma et al.*, Adv. Space Res., **54**, 252, 2014.
27. *M.K.Sharma*, *M.Sharma*, *U.P.Verma et al.*, Adv. Space Res., **55**, 434, 2015.
28. *M.K.Sharma*, *M.Sharma*, *S.Chandra*, Astrophys. Space Sci., **362**, 168, 2017.
29. *M.K.Sharma*, *M.Sharma*, *S.Chandra*, Astrophys. Space Sci., **363**, 94, 2018.
30. *M.K.Sharma*, *M.Sharma*, *S.Chandra*, Mol. Astrophys., **12**, 20, 2018.